

**Spin-lattice interactions through the quantum critical transition in  $\text{Cu}(\text{pyz})(\text{NO}_3)_2$** 

Ö. Günaydın-Şen,<sup>1</sup> C. Lee,<sup>2</sup> L. C. Tung,<sup>3</sup> P. Chen,<sup>1</sup> M. M. Turnbull,<sup>4</sup> C. P. Landee,<sup>4</sup> Y. J. Wang,<sup>3</sup> M.-H. Whangbo,<sup>2</sup> and J. L. Musfeldt<sup>1</sup>

<sup>1</sup>*Department of Chemistry, University of Tennessee, Knoxville, Tennessee 37996, USA*

<sup>2</sup>*Department of Chemistry, North Carolina State University, Raleigh, North Carolina 27695, USA*

<sup>3</sup>*National High Magnetic Field Laboratory, Tallahassee, Florida 32310, USA*

<sup>4</sup>*Carlson School of Chemistry and Department of Physics, Clark University, Worcester, Massachusetts 01610, USA*

(Received 22 January 2010; revised manuscript received 1 March 2010; published 31 March 2010)

We measured the magnetoinfrared response of the quasi-one-dimensional quantum Heisenberg antiferromagnet  $\text{Cu}(\text{pyz})(\text{NO}_3)_2$  to investigate local lattice distortions through the field-driven transition to the fully polarized state. This magnetic quantum critical transition involves changes in the out-of-plane N and C-H bending modes of pyrazine with field that directly track the magnetization. We discuss our findings in terms of calculated spin densities, scaling laws, and extracted spin-phonon coupling constants, the latter of which are large due to the softness of the superexchange ligand.

DOI: [10.1103/PhysRevB.81.104307](https://doi.org/10.1103/PhysRevB.81.104307)

PACS number(s): 75.30.Kz, 68.35.Ja, 75.50.Ee, 78.30.-j

**I. INTRODUCTION**

The discovery that the copper halide coordination polymer  $[\text{Cu}(\text{HF}_2)(\text{pyz})_2]\text{BF}_4$  displays important magnetostructural interactions through the field-driven transition to the fully polarized state<sup>1</sup> is providing important insights into functionality in complex materials. The microscopic lattice response is particularly illuminating because it goes to the heart of both symmetry criteria and mechanisms.<sup>2,3</sup> The challenge is that direct observation of phonons that are sensitive to magnetic state is quite rare, and as a consequence, there are few physical systems with which to evaluate specific local structure changes (i.e., local distortions that change site symmetry, bond lengths, and angles) that accompany magnetically driven transitions.  $[\text{Cu}(\text{HF}_2)(\text{pyz})_2]\text{BF}_4$  was ideal in that it allowed an initial test of these ideas. A more sensitive model compound is, however, needed to extract quantitative information on scaling and coupling constants. Copper pyrazine dinitrate,  $\text{Cu}(\text{pyz})(\text{NO}_3)_2$ , attracted our attention as a system that advantageously combines overall low magnetic energy scales with a cooperative magnetic state, a soft lattice, tunable molecular architecture, and the potential for substantial magnetoelastic coupling. The latter is a consequence of the quasi-one-dimensional structure (and lack of steric constraints), as detailed below. At the same time, the simple chemical and physical structure enables a microscopic analysis that was not possible in quasi-two-dimensional  $[\text{Cu}(\text{HF}_2)(\text{pyz})_2]\text{BF}_4$ .<sup>1</sup> Specifically, we extract a power-law relationship between lattice effects and magnetization, apply traditional scaling models to the data, and calculate spin-lattice coupling constants.

$\text{Cu}(\text{pyz})(\text{NO}_3)_2$  is a quasi-one-dimensional Heisenberg antiferromagnet with small spin-exchange interactions.<sup>4-11</sup> This molecular solid consists of  $\text{Cu}^{2+}$  centers connected by pyrazine rings to form a chain in which the antiferromagnetic (AFM) exchange interactions between magnetic centers are mediated by pyrazine linkages with  $J = -10.3$  K.<sup>4-8,10</sup> Here, we employ a spin Hamiltonian of the form  $-\sum J_{ij} S_i \cdot S_j$ . Nitrate groups separate the copper-pyrazine chains, an arrangement that gives rise to very weak interchain coupling and

hence a very low three-dimensional ordering temperature.<sup>10</sup> Because of these low-energy scales, a powered magnet can drive the system through the magnetic transition.<sup>8,11</sup>  $\text{Cu}(\text{pyz})(\text{NO}_3)_2$  reaches the fully saturated state in an applied field of approximately 15 T at 2 K. The transition regime broadens slightly at 4 K because  $T_N = 0.1$  K.<sup>10</sup> Nevertheless, there is a strong similarity between the 4 and 2 K magnetization curves,<sup>8</sup> demonstrating the well-established fact that spin correlations in low-dimensional antiferromagnets are present well above the long-range magnetic ordering temperature. These short-range correlations are also evidenced as a broad maximum centered around 6.5 K in the susceptibility.<sup>5-7,12,13</sup> Our experiments thus probe low-dimensional spin interactions within the copper-pyrazine chains plus a strong remnant of the long-range ordered state.

In order to investigate spin-lattice coupling in a model one-dimensional quantum Heisenberg antiferromagnet, we measured the magnetoinfrared response of  $\text{Cu}(\text{pyz})(\text{NO}_3)_2$  through the magnetically driven transition to the fully polarized state. Two out-of-plane pyrazine vibrational modes are exquisitely sensitive to applied field, tracking the magnetization through the transition with a  $M \sim [\int \Delta \alpha(d\omega)]^n \sim (\mu_0 H - \mu_0 H_c)^{1/\delta}$  scaling law. The extracted values of  $n$  and  $\delta$  are consistent with decelerating dynamical processes and low-dimensional behavior. Large coupling constants were also observed. Complementary spin-density calculations reveal that out-of-plane pyrazine distortions through the magnetic quantum critical transition occur to reduce the Cu-pyz-Cu spin exchange at high field. The finding that the lattice must relax in a particular way to accommodate the magnetic transition is important for other soft molecular materials as well as higher-energy-scale complex oxides, where powered and pulsed field magnets cannot easily saturate the magnetization.

**II. METHODS**

$\text{Cu}(\text{pyz})(\text{NO}_3)_2$  single crystals were grown by solution techniques<sup>4</sup> and mixed with paraffin or KCl to form isotropic pellets for use in the far and middle infrared, respectively.

Variable-temperature infrared transmittance measurements were done with  $0.5 \text{ cm}^{-1}$  resolution between 4 and 300 K. Absorption was calculated as  $\alpha(\omega) = -\frac{1}{hd} \ln T(\omega)$ , where  $h$  is loading,  $d$  is thickness, and  $T(\omega)$  is the measured transmittance. Magnetoinfrared experiments were carried out at the NHMFL using a 33 T resistive magnet. To better visualize field-induced spectral modifications, we calculated the absorption difference as  $\alpha(H) - \alpha(0 \text{ T})$  and quantified changes in the absolute absorption difference spectra as  $\int |\alpha(H) - \alpha(0)| d\omega$ . Standard partial sum-rule techniques were employed to calculate field-induced changes in oscillator strength as  $\Delta f \equiv \frac{2c}{N_A h \pi \omega_p^2} \int \frac{w_2^2 n \Delta \alpha d\omega}{w_1}$ .<sup>14,15</sup> Spin-density distributions for the AFM and the ferromagnetic (FM) states were calculated using the Vienna *ab initio* simulation package<sup>16–18</sup> with the generalized-gradient approximation,<sup>19</sup> the plane-wave cutoff energy of 400 eV, and a set of 50  $k$  points for the irreducible Brillouin zone.  $U_{\text{eff}} = 4 \text{ eV}$  was employed for the Cu 3d states.<sup>20</sup>

### III. RESULTS AND DISCUSSION

Figure 1 displays the magnetoinfrared response of  $\text{Cu}(\text{pyz})(\text{NO}_3)_2$  at 4.2 K. Panels (a), (c), and (e) show closeup views of the absolute absorption. We assign the  $495 \text{ cm}^{-1}$  doublet and the  $826 \text{ cm}^{-1}$  feature as out-of-plane N and C-H bending modes of pyrazine, respectively.<sup>1,21–23</sup> Schematic displacement patterns are shown in Figs. 2(a) and 2(b). These out-of-plane pyrazine bending modes are very sensitive to field. The striking size and systematic nature of the field-induced vibrational property modifications are emphasized in the absorption difference spectra [Figs. 1(b) and 1(d)]. With increasing field, the out-of-plane N and C-H pyrazine bending modes soften and appear to change intensity. The former is evidenced by the characteristic derivative-like line shape in  $\alpha(H) - \alpha(0 \text{ T})$ . A partial sum-rule analysis<sup>14</sup> reveals that oscillator strength is conserved within our sensitivity, demonstrating that the structure that develops in the absorption difference spectra corresponds to a local redistribution of oscillator strength. At full field (33 T), the  $495 \text{ cm}^{-1}$  out-of-plane N bending mode of pyrazine displays a 77% contrast, and the  $826 \text{ cm}^{-1}$  out-of-plane C-H bending of pyrazine shows a 35% difference.<sup>24</sup> Distinctly different vibrational modes resonate in the  $900\text{--}1700 \text{ cm}^{-1}$  range [Fig. 1(e)]. They include in-plane pyrazine and  $\text{NO}_3^-$  stretching modes,<sup>21–23,25–27</sup> none of which show any field dependence within our sensitivity [Fig. 1(f)]. Low-frequency Cu- $\text{NO}_3$  and Cu-pyz lattice modes (not shown)<sup>22,23</sup> also do not display field-induced spectral changes. Overall, our signal-to-noise ratio is on the order of 0.03% [Fig. 1(g)]. These results demonstrate that the 15 T magnetically driven transition in  $\text{Cu}(\text{pyz})(\text{NO}_3)_2$  is accompanied by substantial magnetoelastic interactions involving only out-of-plane bending modes of the pyrazine ligand.

We quantify changes in the out-of-plane pyrazine bending modes by integrating the absolute value of the absorption difference spectrum,  $\int |\alpha(H) - \alpha(0)| d\omega$ , and plotting the results as a function of magnetic field (Fig. 3). We carried out this analysis for both out-of-plane vibrational modes of pyrazine in  $\text{Cu}(\text{pyz})(\text{NO}_3)_2$ , the  $495 \text{ cm}^{-1}$  out-of-plane N bend

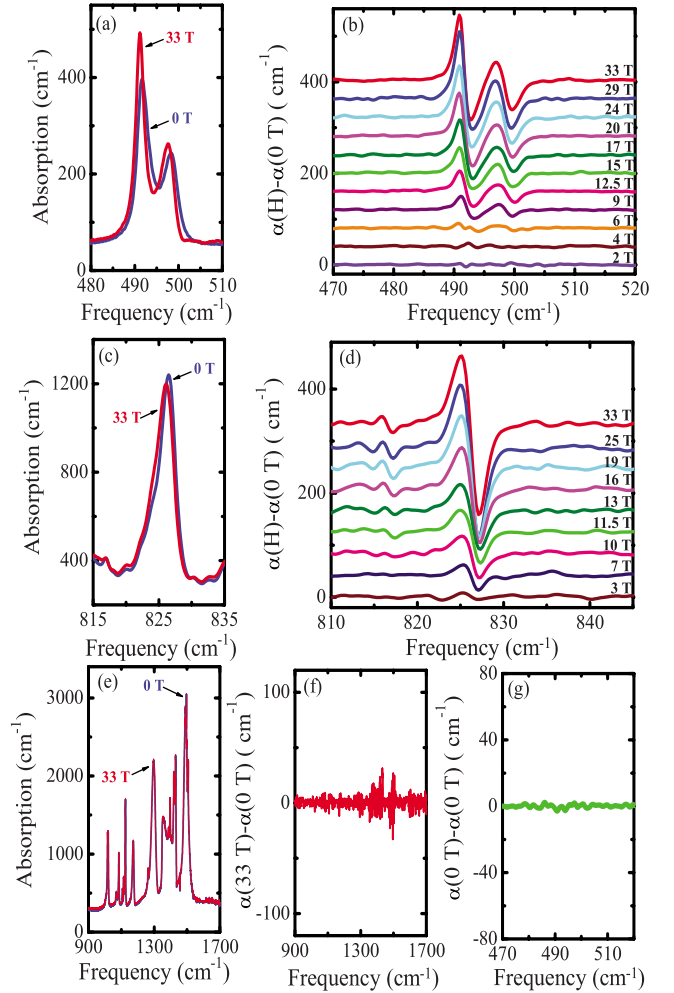


FIG. 1. (Color online) (a), (c), and (e): closeup views of the 4.2 K absolute absorption spectra at 0 and 33 T. (b), (d), and (f): closeup views of the 4.2 K absorption difference spectra,  $\alpha(H) - \alpha(0 \text{ T})$ , in a similar frequency range. Data in (b) and (d) are offset along the y axis by  $40 \text{ cm}^{-1}$  for clarity. (g): closeup view of the 4.2 K absorption difference spectra,  $\alpha(0 \text{ T}) - \alpha(0 \text{ T})$ , illustrating the noise level of our data before and after a field sweep.

and the  $826 \text{ cm}^{-1}$  out-of-plane C-H bend, and compared the results with the low-temperature magnetization.<sup>8</sup> Overall,  $\int |\Delta \alpha| d\omega$  tracks the 4.2 K magnetization remarkably well. It is small at low fields, begins to rise as the spins start to cant, increases through the critical range, and levels off at high field, consistent with magnetization saturation in the fully polarized state. Here and in other copper halides,<sup>1,29</sup> there is a slight delay between the microscopic lattice response (or the optical contrast) and the magnetization, which may have roots in the functional form employed to analyze the spectroscopic response.<sup>30</sup> In the absence of a microscopic model to provide a robust functional form for the field dependence of the lattice response, we turned our attention to some simple variations in the absorption difference and compared the results to the experimental magnetization. Substantially better agreement was obtained using a power-law form for the absorption difference spectra (Fig. 3), indicative of important dynamical processes at the 15 T magnetically driven transition.<sup>31–37</sup> We employed a traditional scaling model of

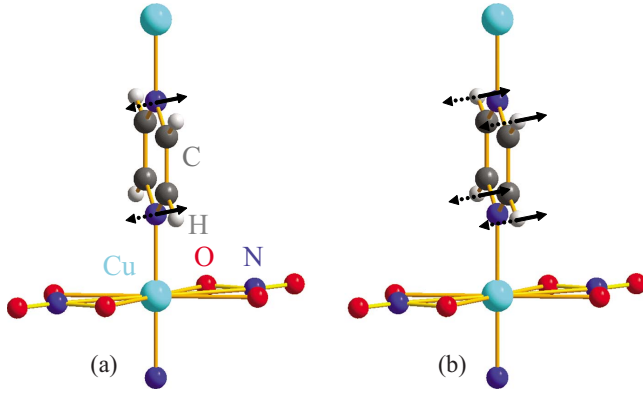


FIG. 2. (Color online) Schematic view of the displacement patterns for the two out-of-plane pyrazine-related vibrational modes in  $\text{Cu}(\text{pyz})(\text{NO}_3)_2$ : (a) out-of-plane N bend of pyrazine and (b) out-of-plane C-H bend of pyrazine.

the form  $M \sim [f|\Delta\alpha|d\omega]^n \sim (\mu_0 H - \mu_0 H_c)^{1/\delta}$  to investigate behavior very close to the transition. Here,  $n$  is the power-law exponent (1.0 or 0.65) and  $\delta$  is the critical exponent. We used existing magnetization data<sup>8</sup> and our  $f|\Delta\alpha|d\omega$  results (with and without the power-law modification) to fit the behavior near the critical field. Both magnetization and the absorption difference data follow this scaling law with  $\delta \approx 1$  near the transition.

For a uniform AFM chain with nearest-neighbor spin exchange  $J$ , the fully spin-polarized FM state is higher in energy than the AFM state by  $\Delta E = 2|J|$  per spin site. The local lattice distortions described above occur in response to the change in magnetic state as a way of lowering the energy of the FM state forced upon the system by external magnetic field. Qualitatively, the AFM exchange  $J$  can be written as  $J = -\frac{4t^2}{U}$ , where  $t$  is the hopping integral between the two Cu

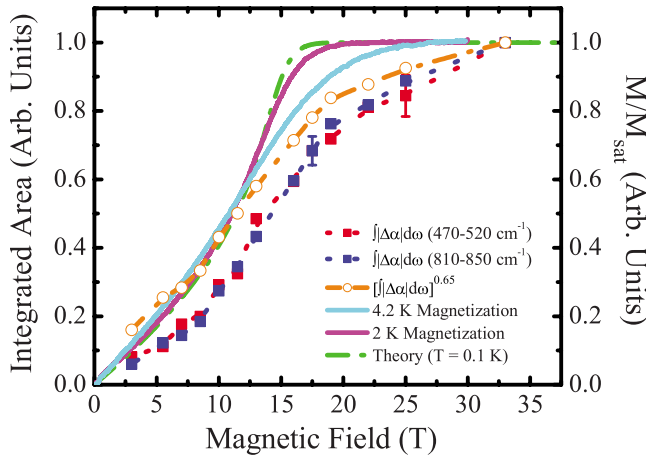


FIG. 3. (Color online) Integrated area of the absolute value of the 4.2 K absorption difference spectra,  $\int |\alpha(H) - \alpha(0)| d\omega$ , and the related power-law data  $[\int |\alpha(H) - \alpha(0)| d\omega]^{0.65}$  as a function of applied field, normalized to the full field value, along with the relative magnetization  $M/M_{\text{sat}}$ , at 4.2 and 2 K (Ref. 8). This comparison demonstrates the relationships between the lattice response and magnetization. Combined Bethe formalism/Monte Carlo simulations were used for the theoretical curve (Refs. 8 and 28).

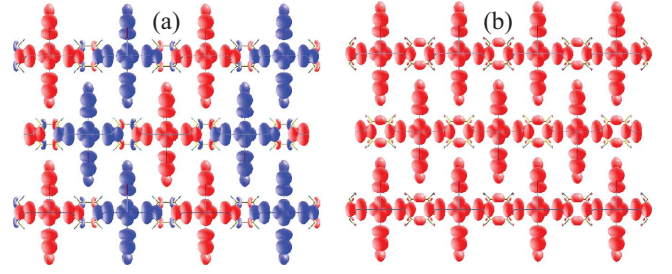


FIG. 4. (Color online) Calculated spin-density distributions for (a) the AFM and (b) the FM states of  $\text{Cu}(\text{pyz})(\text{NO}_3)_2$ . Red (light) and blue (dark) shading indicates different spin densities. Out-of-plane pyrazine ligand distortions reduce AFM coupling in the high-field phase.

sites of the Cu-pyz-Cu spin-exchange path and  $U$  is the on-site repulsion on Cu. Thus, the energy of the FM state can be lowered by reducing the value of  $t$ , which occurs when pyrazine adopts an out-of-plane bent structure. The observed magnetoinfrared effects are strong because the pyrazine ligand is soft toward out-of-plane bending. Figure 4 displays the spin-density plots calculated for the AFM and the FM states of  $\text{Cu}(\text{pyz})(\text{NO}_3)_2$ . Note that, unlike the case of the AFM state, the two carbon atoms in each C-C bond of pyrazine have identical spin densities in the FM state. Such a spin polarization in the C-C bonds of pyrazine is energetically unfavorable, and the extent of this energetically unfavorable situation is reduced by the out-of-plane bending of pyrazine.

Finally, we employed our magnetoinfrared data to estimate the spin-phonon coupling constants. Phonon frequencies are sensitive to spin correlations as  $\omega = \omega_0 + \lambda \langle \mathbf{S}_i \cdot \mathbf{S}_j \rangle$ , where  $\lambda$  is the spin-phonon coupling constant and  $\langle \mathbf{S}_i \cdot \mathbf{S}_j \rangle$  is the nearest-neighbor spin-spin correlation function.<sup>38–41</sup> To extract  $\lambda$ , we estimate  $\langle \mathbf{S}_i \cdot \mathbf{S}_j \rangle$  by relating the spin-spin correlation function to the magnetic specific heat.<sup>40</sup> The relative change in magnetic energy with temperature is given as  $\langle \mathbf{S}_i \cdot \mathbf{S}_j \rangle = \text{const} + \frac{1}{nN_A J} \int_{T_N}^T C_m(T) dT$ , where  $n=1$  is the number of Cu-pyz-Cu superexchange linkages per formula unit,  $N_A = 6.02 \times 10^{23}$  formula units/mol, and  $C_m$  is the magnetic specific heat per mole. Using the data from Hammar *et al.* between 0.1 and 10 K,<sup>8</sup> we find  $\langle \mathbf{S}_i \cdot \mathbf{S}_j \rangle = -0.24$ . We employ this result to calculate the  $\lambda$ 's for the field-dependent vibrational features (Table I). The coupling constants are relatively large (2 or 3  $\text{cm}^{-1}$  depending on the mode), less than those in several magnetically frustrated oxides<sup>3,39–41</sup> but larger than those of chemically similar  $[\text{Cu}(\text{HF}_2)(\text{pyz})_2]\text{BF}_4$ .<sup>1</sup> Absence of steric hindrance effects in the quasi-one-dimensional material thus allows maximum distortion of the pyrazine ligand. The size of these  $\lambda$ 's indicates that the lattice is not rigid through the field-induced transition to the fully polarized state.

#### IV. SUMMARY

To summarize, we employed magnetoinfrared spectroscopy to investigate magnetoelastic effects through the magnetically driven quantum critical transition in the quasi-one-dimensional Heisenberg antiferromagnet  $\text{Cu}(\text{pyz})(\text{NO}_3)_2$ .

TABLE I. Spin-phonon coupling constants,  $\lambda$ , for selected modes of  $\text{Cu}(\text{pyz})(\text{NO}_3)_2$  estimated using  $\langle \mathbf{S}_i \cdot \mathbf{S}_j \rangle \approx -0.24$ . All frequencies, frequency differences, and coupling constants (rounded to the nearest whole number) are in  $\text{cm}^{-1}$ . The large coupling constants demonstrate that the lattice is not rigid in an applied magnetic field.

Mode assignments	$\omega_0$ (0 T, experiment) ( $\text{cm}^{-1}$ )	$\omega$ (33 T, experiment) ( $\text{cm}^{-1}$ )	$\Delta\omega$ ( $\text{cm}^{-1}$ )	$\lambda$ ( $\text{cm}^{-1}$ )
Out-of-plane N bend of pyrazine	491.6	491.2	-0.4	2
Out-of-plane N bend of pyrazine	498.3	497.6	-0.7	3
Out-of-plane C-H bend of pyrazine	826.5	826.1	-0.4	2

Our measurements reveal coupling of two out-of-plane pyrazine distortions to the transition, a process quantified by a scaling law analysis, a power-law fit, and sizeable coupling constants which indicate that this prototypical magnetic transition does not take place in isolation. These findings, demonstrated here in one of the simplest cooperative quantum magnets, are relevant to the fundamental understanding of field-driven magnetic ordering transitions in copper halides. Analogous effects are anticipated to occur in other magnetic materials although due to magnetic energy scale consider-

ations, molecular materials may be most promising for future study.

### ACKNOWLEDGMENTS

This work was supported by the NSF (UT, Clark University, NHMFL), the DOE (NCSSU, NHMFL), and the State of Florida (NHMFL). We thank T. V. Brinzari, A. B. Sushkov, and O. Tchernyshyov for useful discussions.

- <sup>1</sup>J. L. Musfeldt, L. I. Vergara, T. V. Brinzari, C. Lee, L. C. Tung, J. Kang, Y. J. Wang, J. A. Schlueter, J. L. Manson, and M.-H. Whangbo, *Phys. Rev. Lett.* **103**, 157401 (2009).
- <sup>2</sup>A. B. Harris, T. Yildirim, A. Aharony, and O. Entin-Wohlman, *Phys. Rev. B* **73**, 184433 (2006).
- <sup>3</sup>L. I. Vergara, J. Cao, N. Rogado, Y. Q. Wang, R. P. Chaudhury, R. J. Cava, B. Lorenz, and J. L. Musfeldt, *Phys. Rev. B* **80**, 052303 (2009).
- <sup>4</sup>A. Santoro, A. D. Mighell, C. W. Reimann, *Acta Crystallogr., Sect. B: Struct. Crystallogr. Cryst. Chem.* **26**, 979 (1970).
- <sup>5</sup>W. E. Hatfield and J. F. Villa, *J. Am. Chem. Soc.* **93**, 4081 (1971).
- <sup>6</sup>D. B. Losee, H. W. Richardson, and W. E. Hatfield, *J. Chem. Phys.* **59**, 3600 (1973).
- <sup>7</sup>G. Mennenga, L. J. De Jongh, and W. J. Huiskamp, *J. Magn. Magn. Mater.* **44**, 89 (1984).
- <sup>8</sup>P. R. Hammar, M. B. Stone, D. H. Reich, C. Broholm, P. J. Gibson, M. M. Turnbull, C. P. Landee, and M. Oshikawa, *Phys. Rev. B* **59**, 1008 (1999).
- <sup>9</sup>M. B. Stone, D. H. Reich, C. Broholm, K. Lefmann, C. Rischel, C. P. Landee, and M. M. Turnbull, *Phys. Rev. Lett.* **91**, 037205 (2003).
- <sup>10</sup>T. Lancaster, S. J. Blundell, M. L. Brooks, P. J. Baker, F. L. Pratt, J. L. Manson, C. P. Landee, and C. Baines, *Phys. Rev. B* **73**, 020410(R) (2006).
- <sup>11</sup>A. V. Sologubenko, K. Berggold, T. Lorenz, A. Rosch, E. Shishoni, M. D. Phillips, and M. M. Turnbull, *Phys. Rev. Lett.* **98**, 107201 (2007).
- <sup>12</sup>A. B. Kuz'menko, D. van der Marel, P. J. M. van Bentum, E. A. Tishchenko, C. Presura, and A. A. Bush, *Phys. Rev. B* **63**, 094303 (2001).
- <sup>13</sup>L. J. de Jongh and A. R. Miedema, *Adv. Phys.* **23**, 1 (1974); **50**, 947 (2001).
- <sup>14</sup>F. Wooten, *Optical Properties of Solids* (Academic Press, New York, London, 1972).
- <sup>15</sup>Here,  $N_e$  is the effective number of electrons,  $n=1.5$  is the refractive index,  $\omega_p$  is the plasma frequency  $\equiv \sqrt{\frac{e^2 \rho}{m \epsilon_0}}$ , where  $\rho$  is the density of  $\text{Cu}(\text{pyz})(\text{NO}_3)_2$ ,  $e$  and  $m$  are the charge and mass of an electron,  $\epsilon_0$  is the vacuum dielectric constant,  $\rho$  is the density of  $\text{Cu}(\text{pyz})(\text{NO}_3)_2$ ,  $c$  is the speed of light, and  $\omega_1$  and  $\omega_2$  are the frequencies of integration.
- <sup>16</sup>P. E. Blöchl, *Phys. Rev. B* **50**, 17953 (1994).
- <sup>17</sup>G. Kresse and D. Joubert, *Phys. Rev. B* **59**, 1758 (1999).
- <sup>18</sup>G. Kresse and J. Furthmüller, *Phys. Rev. B* **54**, 11169 (1996).
- <sup>19</sup>J. P. Perdew, K. Burke, and M. Ernzerhof, *Phys. Rev. Lett.* **77**, 3865 (1996).
- <sup>20</sup>S. L. Dudarev, G. A. Botton, S. Y. Savrasov, C. J. Humphreys, and A. P. Sutton, *Phys. Rev. B* **57**, 1505 (1998).
- <sup>21</sup>K. B. Hewett, M. H. Shen, C. L. Brummel, and L. A. Philips, *J. Chem. Phys.* **100**, 4077 (1994).
- <sup>22</sup>B. R. Jones, P. A. Varughese, I. Olejniczak, J. M. Pigos, J. L. Musfeldt, C. P. Landee, M. M. Turnbull, and G. L. Carr, *Chem. Mater.* **13**, 2127 (2001).
- <sup>23</sup>S. Brown, J. Cao, J. L. Musfeldt, M. M. Conner, A. C. McConnell, H. I. Southerland, J. L. Manson, J. A. Schlueter, M. D. Philips, M. M. Turnbull, and C. P. Landee, *Inorg. Chem.* **46**, 8577 (2007).
- <sup>24</sup>Percent contrast was obtained from  $\frac{\alpha(33 \text{ T}) - \alpha(0 \text{ T})}{\alpha(0 \text{ T})}$  vs frequency plots.
- <sup>25</sup>F. Billes, H. Mikosch, and S. Holly, *J. Mol. Struct.: THEOCHEM* **423**, 225 (1998).
- <sup>26</sup>R. V. Biagetti, W. G. Bottjer, and H. M. Haendler, *Inorg. Chem.* **5**, 379 (1966).
- <sup>27</sup>P. M. Castro and P. W. Jagodzinski, *J. Chem. Phys.* **96**, 5296 (1992).
- <sup>28</sup>R. B. Griffiths, *Phys. Rev.* **133**, A768 (1964).

- <sup>29</sup>J. L. White, C. Lee, Ö. Günaydın-Şen, L. C. Tung, H. M. Christen, Y. J. Wang, M. M. Turnbull, C. P. Landee, R. D. McDonald, S. A. Crooker, J. Singleton, M.-H. Whangbo, and J. L. Musfeldt, *Phys. Rev. B* **81**, 052407 (2010).
- <sup>30</sup>The lack of hysteresis rules out a slow lattice relaxation.
- <sup>31</sup>That our best-fit power-law exponent (0.65) is less than one indicates a negatively accelerating or slightly contractive function. Systems with the same critical exponent scale identically on approach to criticality and thus share the same fundamental dynamics.
- <sup>32</sup>S. Sachdev, *Quantum Phase Transitions* (Cambridge University Press, Cambridge, England, 1999).
- <sup>33</sup>B. Lake, D. A. Tennant, C. D. Frost, and S. E. Nagler, *Nature (London)* **4**, 329 (2005).
- <sup>34</sup>S. E. Sebastian, P. A. Sharma, M. Jaime, N. Harrison, V. Correa, L. Balicas, N. Kawashima, C. D. Batista, and I. R. Fisher, *Phys. Rev. B* **72**, 100404(R) (2005).
- <sup>35</sup>B. C. Watson, V. N. Kotov, M. W. Meisel, D. W. Hall, G. E. Granroth, W. T. Montfrooij, S. E. Nagler, D. A. Jensen, R. Backov, M. A. Petruska, G. E. Fanucci, and D. R. Talham, *Phys. Rev. Lett.* **86**, 5168 (2001).
- <sup>36</sup>T. Sakai and M. Takahashi, *Phys. Rev. B* **57**, R8091 (1998).
- <sup>37</sup>K. Li, L. Liu, J. Sun, X. J. Xu, J. Fang, X. W. Cao, J. S. Zhu, and Y. H. Zhang, *J. Phys. D* **29**, 14 (1996).
- <sup>38</sup>D. J. Lockwood and M. G. Cotton, *J. Appl. Phys.* **64**, 5876 (1988).
- <sup>39</sup>C. J. Fennie and K. M. Rabe, *Phys. Rev. Lett.* **96**, 205505 (2006).
- <sup>40</sup>A. B. Sushkov, O. Tchernyshyov, W. Ratcliff II, S. W. Cheong, and H. D. Drew, *Phys. Rev. Lett.* **94**, 137202 (2005).
- <sup>41</sup>J. Cao, L. I. Vergara, J. L. Musfeldt, A. P. Litvinchuk, Y. J. Wang, S. Park, and S.-W. Cheong, *Phys. Rev. B* **78**, 064307 (2008).